Selective Recovery of Precious Metals through Photocatalysis

Yao Chen[1], Mengjiao Xu[1], Jieya Wen[1], Yu Wan[1], Qingfei Zhao[1], Xia Cao[3], Yong Ding[4], Zhong Lin Wang[3,4*], Hexing Li[1,2*] & Zhenfeng Bian[1*]

[1] MOE Key Laboratory of Resource Chemistry and Shanghai Key Laboratory of Rare Earth Functional Materials, Shanghai Normal University, Shanghai 200234, China.

[2] Shanghai University of Electric Power, Shanghai 200090, China.

[3] Beijing Institute of Nanoenergy and Nanosystems, Chinese Academy of Sciences, Beijing 100083, China.

[4] School of Materials Science and Engineering, Georgia Institute of Technology, Atlanta, Georgia 30332-0245, United States.

Precious metals such as gold and platinum are valued materials for a variety of important applications, but their scarcity poses a risk of supply interruption. However, the dissolution and recovery of precious metals using the current methods are limited by associated serious environmental pollution and high energy consumption. Here, we show a photocatalytic process that allows one to selective retrieve 7 kinds of precious metal elements (Ag, Au, Pd, Pt, Ru, Rh and Ir) (with dissolution efficiency of 99%) from waste circuit boards, ternary automotive catalysts and even ores. Precious metals is recovered with high purity (≥98%) through a simple reductive method. The whole process only needs light and catalyst without strong acid, strong base and highly toxic cyanide. It has an environmentally friendly, scalable and efficient way, in which the catalyst has been recycled more than 100 times under normal temperature and pressure without performance degradation. It has successfully realized the scale of dissolution from grams to kilograms, and it is expected to realize large-scale recovery of precious metals in industrial application. This general approach provides an unprecedent technology for recycling resources on earth.

Introduction

Precious metals (PMs) possess not only good physical properties (ductility, electrical conductivity), but also high chemical stability and strong corrosion resistance[1]. In recent years, precious metals have been increasingly used in the fields of electronic devices and modern industrial catalysis[2,3] etc. It is reported that the global demand for gold, silver and palladium in the electronics industry was about 250 tons, 12,800 tons and 40 tons, respectively[4-6]. In addition, due to the continuous development of the automobile industry, the consumption of platinum group metals is increasing[5]. The global electronic waste (e-waste) production shows that the gold content in 40 mobile phones is equivalent to one ton of ore[7]. In 2019, a total of 53.6 million tons of precious metal-containing e-waste were generated globally, including discarded computers, mobile phones and households electronic equipment[8,9]. It is a very meaningful to recycle precious metals from e-waste and waste catalyst.

It remains a grand challenge to mine and retrieve precious metals from ores, catalysts and electronic wastes for reusage[10-13]. The recovery process of precious metal is divided into two steps: firstly, dissolve PM^0 into PM^{x+} from electronic wastes; then reduce PM^{x+} to PM^0 from the leachate. In the process of dissolving PM^0 to PM^{x+}, dissolution methods in the industry involving the use of corrosive and toxic aqua regia and cyanidation endanger the environment and characterized of high chemical consumption[14-18]. In view of the toxicity of aqua regia and cyanide, scientists have developed non-toxic leaching agents such as thiourea, thiosulfate and iodine to treat the dissolution of gold, but they are ineffective for the dissolution of platinum group precious metals and the operation steps are complicated (Extended Data Table 1)[18-23]. Moreover, Yang et al. used n-bromosuccinimide (NBS) and pyridine (Py) directly leached Au^0 waste to form Au^{III} from gold ore and electronic[24]. Hong et al. used sulfuryl chloride ($SOCl_2$) and some organic solvents/reagents (pyridine, N, N-dimethylformamide and imidazole) to form "organic aqua regia" to dissolve gold and palladium[25]. The limitation of the above method is that it can only dissolve one or two precious metals and the reagent composition is complicated, which not only increases

the difficulty of actual operation, but also increases the cost of recovery. In the process of reducing PM^{x+} to PM^0, scientists usually design materials that can withstand acid to extract precious metal ions. Hong et al. reported a porous porphyrin polymer which can quantitatively capture precious metals ion from the acidic exudate of e-waste[26]. The existing methods in the literature can achieve selective reduction of a precious metal. Smith et al. used 1,3:2,4-dibenzylidenesorbitol as a raw material to prepare a hydrogel material capable of extracting gold/silver ions[27]. Queen et al. prepared Fe-BTC/PpPDA composite material, which was proven to quickly extract trace amounts of gold ion from water mixtures[28]. In fact, the dissolution process of precious metals is more difficult to achieve than reduction because precious metals are chemically inert, which require strong oxidizing reagents.

It has been reported that the photocatalysis can generate highly reactive free radicals in the reaction system under mild conditions. Moreover, the photocatalytic technology has the advantages of simple operation, low energy consumption, no secondary pollution and high efficiency. Photocatalytic oxidation has become a technology of choice to tackle environmental pollution and energy crisis due to its direct utilization of solar light-driven reaction and good catalyst stability. The oxidizing ability of photo-generated holes (TiO_2 (2.91 V_{NHE})) is sufficient to oxidize PM^0 into PM^{x+} (Rh (0.75 V_{RHE}) < Ir (0.9 V_{RHE}) < Pt (1.1 V_{RHE}) < Au (1.3 V_{RHE})) [29,30]. But so far, there is no report on the oxidation and dissolution of precious metals by photocatalytic method.

Here, we have realized the use of photocatalysis to dissolve precious metals, without strong acids, strong bases and toxic solvents. It has good leaching effect for 7 kinds of precious metals (Ag, Au, Pd, Pt, Ru, Rh and Ir). Interestingly, selective dissolution of precious metals can also be achieved, providing an easy way of separating these metals. More importantly, this photocatalytic technology for dissolving precious metals can not only realize the recovery of noble metal nano-catalysts in the laboratory, but also effectively leached precious metals from e-waste, ore and automobile three-way catalyst on a large scale. To our best knowledge, this is

the first time that an environmental friendly photocatalysis has been applied to the dissolution and recovery of precious metals.

Results

Photocatalytic Dissolution of Precious Metals

Here, photocatalysis was used to recycle precious metals from waste electrical and electronic equipment (WEEE), ore waste and three-way catalytic (TWC). As shown in **Fig. 1**, gold (Au) from central processing unit (CPU) board (**Fig. 1a-1c**) and gold ore (**Fig. 1d-1f**) was successfully dissolved by light irradiation, as well as palladium (Pd), platinum (Pt) and rhodium (Rh) contained in TWC (**Fig. 1g–1i**). The required reaction conditions are mild and the raw materials can be simply added and mixed (**Extended Data Fig. 1**). By crushing the bulk samples, the reaction contact surface can be increased and more metals will be dissolved out (**Extended Data Fig. 2**). As shown in **Extended Data Fig. 3**, there are several metals such as copper (Cu), nickel (Ni) and gold (Au) in the CPU board. In the process of photocatalytic dissolution, these non-noble metals can also be dissolved (**Extended Data Fig. 4)**. Compared with the aqua regia method, the photocatalytic process has a mild reaction. The dissolution process of aqua regia reacts violently and produces a large amount of toxic and harmful substances, such as chlorine. The fracture of CPU block was seriously cracked (**Extended Data Fig. 5**).

Scalability Dissolution of Precious Metals

The whole dissolution process is very simple, and the scale of the experiment can be easily increased to the kilogram level. Take CPU and gold ore as examples (**Fig. 1j–1o**), we used 1.137 kg of CPU board and 1.169 kg of ore respectively. With the increase of reaction time, the content of gold in the solution increased gradually. The color of the solution showed the yellow characteristic of gold ions. These showed that the method is feasible in scale-up.

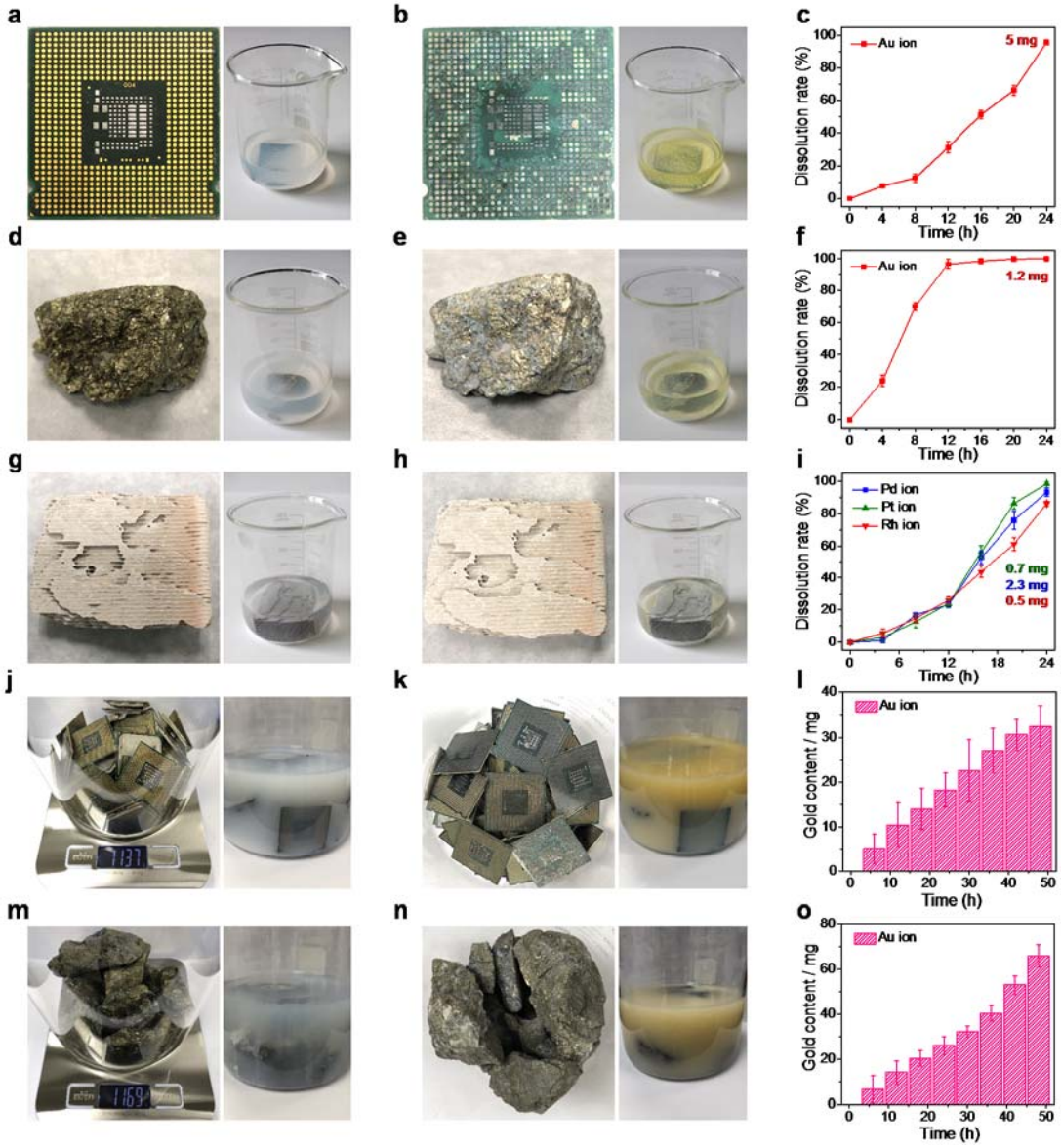

112

113 **Figure 1 | Photocatalytic dissolution of precious metals from CPU board, gold ore**
114 **and TWC.** Photographs of retrieving gold from CPU board (a) before and (b) after
115 reaction. Photographs of retrieving gold from gold ore (28.8 g) (d) before and (e) after
116 reaction. Photographs of retrieving precious metals from TWC (17.9 g) (g) before and
117 (h) after reaction. Photographs of retrieving gold from CPU board (1.137 kg) (j) before
118 and (k) after reaction. Photographs of retrieving gold from ore (1.169 kg) (m) before
119 and (n) after reaction. The amount of precious metals obtained by photocatalyzing
120 unbroken CPU board (c) (l), gold ore (f) (o) and TWC (i).

121

Selective Dissolution of Precious Metals

We investigated the dissolution rate of different solvents for different metals under photocatalytic conditions. In the mixed system of acetonitrile (MeCN) and dichloromethane (DCM), 7 kinds of precious metals (Au, Ag, Pd, Pt, Ru, Rh and Ir) can be effectively dissolved under light irradiation **(Fig. 2a and Extended Data Fig. 6**). While only Au, Ag and Cu can be dissolved in MeCN under the same conditions. **(Fig. 2b**). Through screening 9 kinds of common solvents, it is found that only MeCN can be used as solvent to realize this dissolution process (**Fig. 2c**). The selective dissolution of precious metals was achieved by adjusting the reaction solvent and reaction time. Taking the CPU board as the research object, the results showed that Cu, Ag and Au on CPU board dissolved step by step with the increase of irradiation time (**Fig. 2d-2e**).

To evaluate the selectivity of photocatalytic dissolution, TiO_2 samples loaded with commonly used metals Cu, Ag, Au and Pt were selected as the research object. As shown in **Figure 2f and 2g**, we sequentially dissolved Cu, Ag and Au in MeCN by controlling the reaction time, then Pt is further dissolved by adding DCM. Finally, we choose the e-waste powder, which contains Fe, Ni, Cu, Ag, Au and Pd. By adjusting the solvent and reaction time, we can selectively recover the precious metals Ag, Au and Pd (**Fig. 2h-2i**).

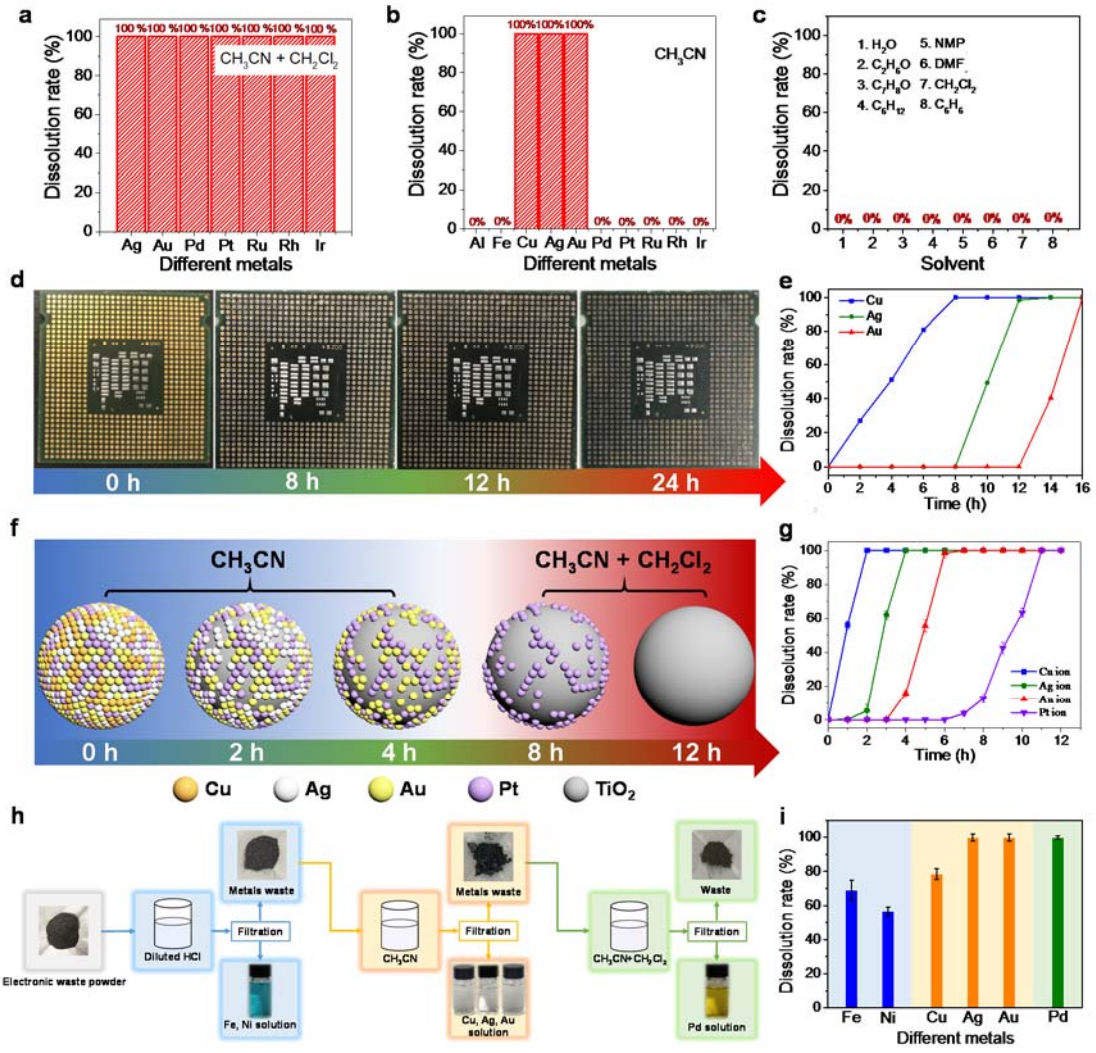

Figure 2 | Photocatalytic selective dissolution of metals. (a) Dissolution rate of Ag, Au, Pd, Pt, Ru, Rh and Ir in the mixed system of MeCN and DCM under photocatalytic conditions. (b) Dissolution rate of Al, Fe, Cu, Ag, Au, Pd, Pt, Ru, Rh and Ir in MeCN under photocatalytic conditions. (c) Dissolution rate of Au in different solution. (d) Photographs of selective retrieving metal from CPU board. (f) Schematic diagram of selective dissolution process of metals catalyst (1% Cu/TiO_2, 1% Ag/TiO_2, 1% Au/TiO_2 and 1% Pt/TiO_2). (h) Flow-sheet of stepwise extraction of Fe, Ni, Cu, Ag, Au and Pd from e-waste powder. The amount of metals obtained by selective photocatalyzing (e) CPU board, (g) metals catalyst and (i) e-waste powder.

Reduction Recovery of Precious Metal Ion

There are many ways to reduce PM^{x+} to PM^{0}, such as hydrogen reduction, thermal reduction, and reducing agents. Here, we choose the simplest hydrogen reduction method, which can directly obtain the precious metals. The reduction process is divided into two steps: the first is to recycle the solvent, and the second is to reduce the precipitated solid to the precious metal. (**Fig. 3a-3d**). The analysis shows that the purity of the recovered precious metals is more than 98% (**Fig. 3e-3h**). Scanning electron microscopy (SEM) shows that the precious metals are nanoparticles (**Fig. 3i-3l**). X-ray diffraction (XRD) further proved that these samples were metal Ag, Au, Pt and Pd, respectively (**Fig. 3m-3p**).

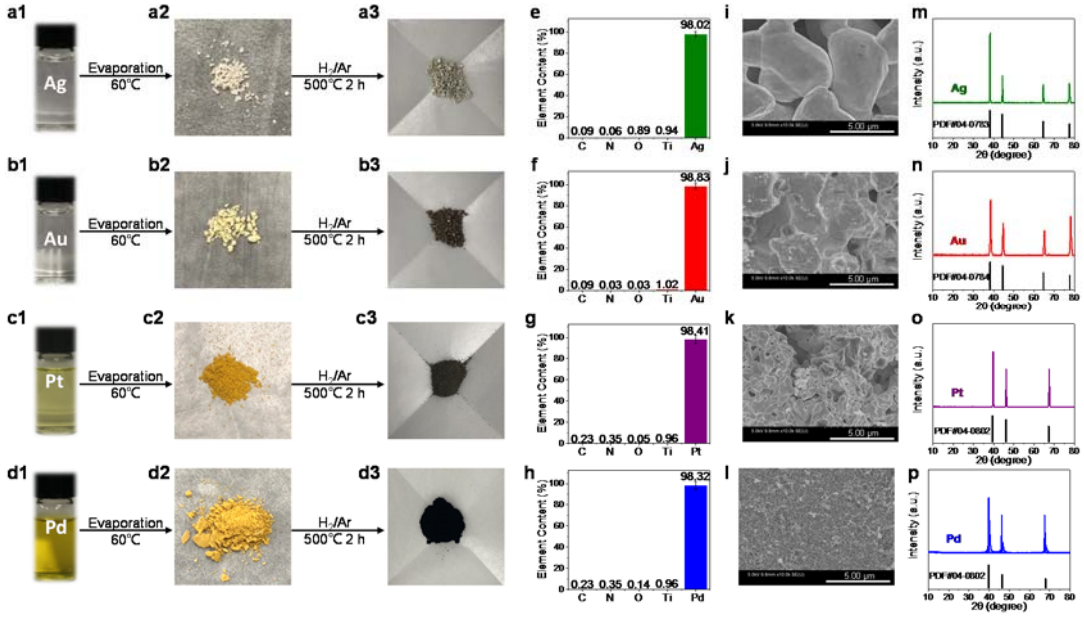

Figure 3 | Precious metal ion reduction process. The solvent of the dissolved product is removed and then calcined in a reducing atmosphere to obtain metal (**a**) Ag, (**b**) Au, (**c**) Pt and (**d**) Pd. The proportion of metal elements in the (**e**) Ag, (**f**) Au, (**g**) Pt and (**h**) Pd after roasting. SEM image of the reduced product (**i**) Ag, (**j**) Au, (**k**) Pt and (**l**) Pd. XRD pattern of the reduced product (**m**) Ag, (**n**) Au, (**o**) Pt and (**p**) Pd.

Discussion

In order to understand the mechanism of photocatalytic dissolution of precious metals, some controlled experiments have been conducted. A commercial 5% Pt/C

sample is used first for photocatalyzing precious metals dissolution. Photocatalysts (TiO_2) and precious metal catalysts (5% Pt/C) are directly mixed in solvents and stirred (**Extended Data Fig. 7**). As shown in **Fig. 4a**, Pt nanoparticles are evenly distributed on carbon surface. Pt nanoparticles disappeared from the surface after UV light illumination (**Fig. 4b**). This can be further analyzed based on the analysis of the elements in the solution, which shows that the content of Pt gradually increases in the solution and Pt is completely dissolved after 4 hours (**Fig. 4g**, red line). The change of Pt content on the surface was further analyzed by XPS spectra[23]. As the reaction proceeded, the binding energies of Pt^0 4*f* dropped substantially (**Fig. 4c**)[31]. To further analyze the structure of the product, we removed the solvent from the reaction solution (after reaction 4 h) and extracted the luminous the yellow powder sample (**Extended Data Fig. 8a**). The infrared spectrum of the powder extracted from the solution after the reaction confirmed the formation of new materials species (**Fig. 4d**). By comparing the infrared spectra of the solution after the reaction, a new infrared absorption peak appeared in the powder sample, located in the region of 3344–2913 cm^{-1}, which is a typical N–H stretching vibration peak[32]. Moreover, the original C-N peak disappeared, which indicates that MeCN can react to form a substance containing N-H bond during the dissolution process[33]. X-ray diffraction (XRD) analysis of powder samples showed that the diffraction of ($(NH_4)_xPtCl_y$) sample has the hexachloroplatinate structure ($(NH_4)_2PtCl_6$) (PDF#07-0218)) (**Fig. 4e**). Compared with the commercial $(NH_4)_2PtCl_6$, the powder samples have similar colors and XRD peak shapes (**Extended Data Fig. 8b-8c**). The N-H peak in powder infrared should be the amino vibration peak in this sample. Energy disperse spectroscopy (EDS) mapping analysis demonstrated that there were only three elements (N, Cl, Pt) in powder samples (**Extended Data Fig. 9**), which is consistent with the results of XRD. X-ray photoelectronic spectroscopy (XPS) analysis further showed that the valence states of platinum in the sample were mainly tetravalent and divalent (Pt^{4+} (73.4 eV and 75.3 eV) and Pt^{2+} (76.7 eV and 78.6 eV)) (**Fig. 4f**)[34]. The N and Cl elements also exhibit corresponding peaks of N-H and Pt-Cl (**Extended Data Fig. 10**). Through electron paramagnetic resonance (EPR) test of the solution, the valence states of platinum in the sample might also have a small amount

of Pt^{+} or Pt^{3+} (**Extended Data Fig. 11**)[35]. From the valence state of Pt, it shows that Pt has been oxidized from Pt^{0} to Pt^{4+}.

Platinum nanoparticles (Pt NPs) on different supports (SiO_2, Al_2O_3 and molecular sieve) can be dissolved by photocatalytic technology (**Extended Data Fig. 12**). The main function of the TiO_2 is to produce active species under light irradiation. Other photocatalysts, such as ZnO (under UV light irradiation) or CdS (under visible light irradiation), can also realize the dissolution of Pt NPs (**Extended Data Fig. 13**). Through the study of the content and change of various solvents, it indicates the importance of cyano group and chloric substituent (**Extended Data Fig. 14**). The aqueous solution of ammonium chloride cannot dissolve Pt NPs through photocatalytic technology, and the inorganic chloride is also ineffective for the dissolution of Pt NPs (**Extended Data Fig. 15**). The control experiments indicate that the presence of oxygen, UV light, and photocatalyst is essential for Pt NPs dissolution (**Fig. 4g**). According to the dissolution efficiency of capturing electrons (the superoxide radicals ($\bullet O_2^-$) formed by the combination with oxygen) and holes (**Fig. 4h**), the photogenerated electrons and holes are the main active charge carriers.

In addition, the $\bullet O_2^-$ and methyl radicals ($\bullet CH_2R$) generated during the reaction were further verified by ESR test (**Extended Data Fig. 16a**). Under the condition of no photocatalyst, free radical is not detected (**Extended Data Fig. 16b**). Further, the content of hydrogen peroxide (H_2O_2) in the system was not detected by the iodometric method, proving that the superoxide radical has not been converted to H_2O_2 (**Extended Data Fig. 17)**. Through a comprehensive analysis of the dissolution system, acetylene was found in the gas phase (**Extended Data Fig. 18**). The experiments of discolored silica gel were used to prove that there was water in the solution after reaction, and the water content in the dissolution reaction is quantitatively detected by Karl Fischer analysis. (**Extended Data Fig. 19**).

Based on the above results, the reaction mechanism of the photocatalyzing dissolution process is proposed in **Fig. 4i**. Photogenerated electrons and holes on TiO_2 are first excited by UV light (stage 1). Photogenerated electrons react with oxygen

molecules to form $\bullet O_2^-$ (stage 2)[36]. Holes react with MeCN in mixed solvents to deprotonate into •CHCN radical (stage 2). DCM decomposes into $\bullet CH_2Cl$ with strong oxidizing ability under the excitation of light (stage 3). These active species oxidize PM^0 to form PM^{x+} (stage 4). At the same time, the solvent is decomposed into acetylene, amino group and water. Finally, the ions coordinate with each other to form $(NH_4)_xPMCl_y$ (stage 5). The dissolved products of Cu and Au also have similar compound structures, which further verifies the reliability of the mechanism. The XPS spectra of Cu and Au show that the metal is ionized after dissolution (**Extended Data Fig. 20a and 20b**). The XRD patterns of Cu compound correspond ammonium chlorocuprate ($(NH_4)_2CuCl_4 \cdot 2H_2O$) (**Extended Data Fig. 20c**). It can be shown that the Au product should be $(NH_4)_xAuCl_y$ by data fitting (**Extended Data Fig. 20d**). The oxidation potential and coordination environment were changed by the regulation of solvent. Therefore, the selective dissolution of Cu, Ag and Au in MeCN can be realized by adjusting the solvent.

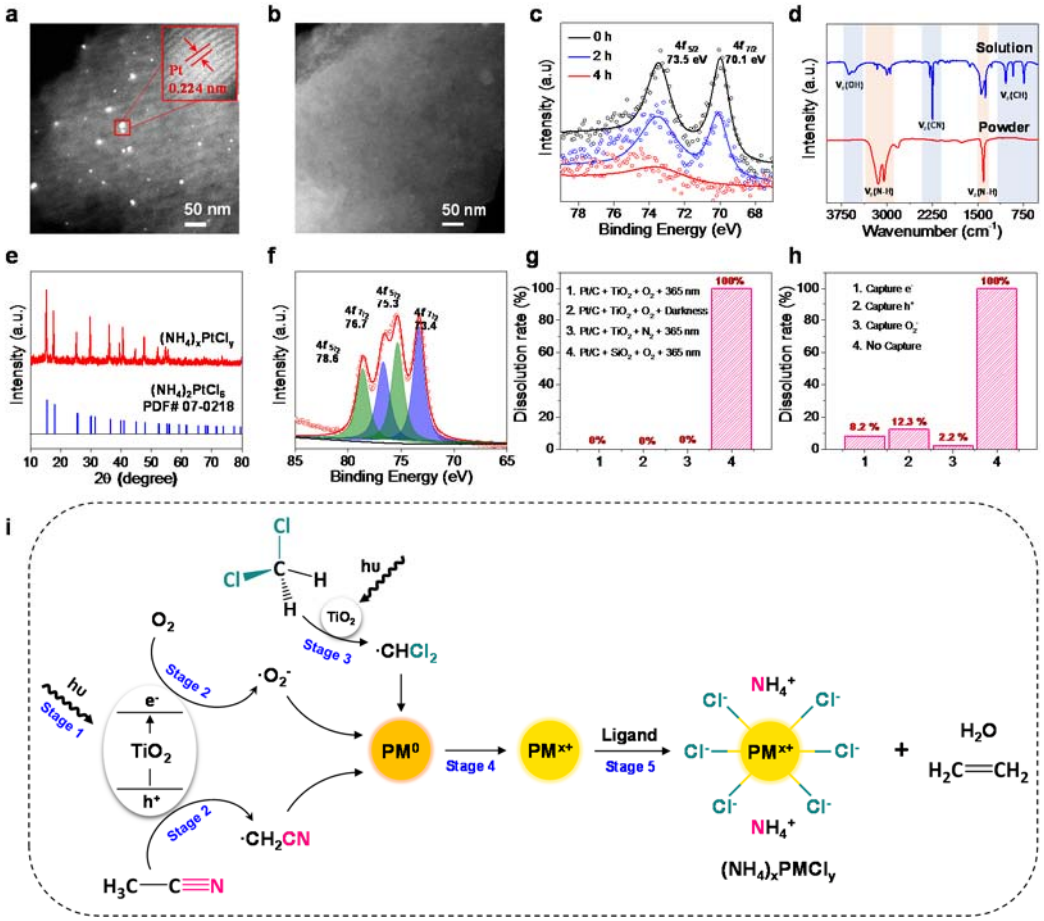

Figure 4 | Exploration of mechanism. High-angle annular dark-field (HAADF) scanning transmission electron microscopy (STEM) images of 5% Pt/C (a) before and (b) after reaction. (c) The Pt element distribution in Pt/C sample determined by XPS spectra with reaction time. (d) FTIR spectra of solution and powder sample after reaction. (e) XRD patterns and (f) Pt 4*f*7 XPS spectra of Pt compound obtained from the solution. (g) Dissolution rate of Pt under different conditions. (h) Dissolution rate of Pt under the capture of different living species (DDQ capture electrons (e^-), EDTA-2Na capture holes (h^+), p-benzoquinone capture superoxide radical ($\bullet O_2^-$)). (i) Proposed mechanism for the retrieving precious metal by photocatalysis.

In this work, we are able to take the advantage of the photocatalytic oxidation technology to solve the complete and selective dissolution of precious metals under mild conditions. We realized the oxidation leaching of precious metal ions from e-waste, ore and TWC, and then recovered the precious metals. The method is simple, mild and environmentally friendly, and is suitable for all kinds of precious metals. It indicated that the whole reaction process is stable and can be recycled. The reaction solvent can be continuously circulated for more than 45 times (**Extended Data Fig. 21**). In addition, the photocatalyst can be recycled more than 100 times (**Extended Data Fig. 22a**). The morphology and structure of the photocatalyst did not change before and after the reaction (**Extended Data Fig. 22b and 22c**), and no free form of Ti ions was detected in the solution after dissolution (**Extended Data Fig. 22d**). Such a general method has a wide range of applications and can be applied not only to the recovery of precious metals from powder nanocatalysts, but also the recovery of precious metals from WEEE, mining of precious metals ores and TWC. It provides a breakthrough solution for the smelting, dissolution and recovery of precious metals, and broadens the application field of photocatalysis.

Data availability

The data supporting the findings of the study are available within the paper and its Supplementary Information.

References

1. Fan, Z. & Zhang, H. Crystal phase-controlled synthesis, properties and applications of noble metal nanomaterials. *Chem. Soc. Rev.* **45**, 63-82 (2016).
2. Zhao, M. *et al.* Metal-organic frameworks as selectivity regulators for hydrogenation reactions. *Nature* **539**, 76-80 (2016).
3. Sean T. Hunt *et al.* Self-assemblyofnoble metal monolayers ontransition metal carbide nanoparticle catalysts. *Science* **352**, 947-978 (2019).
4. USGS, Commodity Statistics and Information, 2017. https://minerals.usgs.gov/minerals/pubs/commodity/.
5. Li, B. *et al.* Recovery of platinum group metals from spent catalysts: A review. *Int. J. Miner. Process.* **145**, 108-113 (2015).
6. NIMS (National Institude for Material Science, Japan), 2015. Available at: www.nims.go.jp/jpn/news/press/pdf/press215_2.pdf.
7. Cafer T. Yavuz *et al.* Gold Recovery from E‑Waste by Porous Porphyrin−Phenazine Network Polymers. *Chem. Mater.***32,** 5343-5349 (2020).
8. Liu, C. *et al.* Economic and environmental feasibility of hydrometallurgical process for recycling waste mobile phones. *Waste Manage*. **111**, 41-50 (2020).
9. Prudence Dato. Economic analysis of e-waste market. *Int Environ Agreements*. **17**, 815-837 (2017).
10. Doidge, E. D. *et al.* A simple primary amide for the selective recovery of gold from secondary resources. *Angew. Chem. Int. Ed.* **55**, 12436-12439 (2016).
11. Sun, D. T., Gasilova, N., Yang, S., Oveisi, E. & Queen, W. L. Rapid, selective extraction of rrace amounts of gold from complex water mixtures with a metal-organic framework (MOF)/polymer composite. *J. Am. Chem. Soc.* **140**, 16697-16703 (2018).

12. Liu, Z. *et al.* Selective isolation of gold facilitated by second-sphere coordination with alpha-cyclodextrin. *Nat. Commun.* **4**, 1855 (2013).
13. Yue, C. *et al.* Environmentally benign, rapid, and selective extraction of gold from ores and waste electronic materials. *Angew. Chem. Int. Ed.* **56**, 9331-9335 (2017).
14. Cherevko, S. *et al.* Dissolution of noble metals during oxygen evolution in acidic media. *ChemCatChem* **6**, 2219-2223 (2014).
15. McGivney, E. *et al.* Biogenic cyanide production promotes dissolution of gold nanoparticles in soil. *Environ. Sci. Technol.* **53**, 1287-1295 (2019).
16. Birich, A., Stopic, S. & Friedrich, B. Kinetic investigation and dissolution behavior of cyanide alternative gold leaching reagents. *Sci Rep* **9**, 7191 (2019).
17. Ahtiainen, R. & Lundström, M. Cyanide-free gold leaching in exceptionally mild chloride solutions. *J. Clean Prod.* **234**, 9-17 (2019).
18. James Hutton: father of modern geology, *Nature* **119**, 1726–1797 (1927).
19. Lee, H., Molstad, E. & Mishra, B. Recovery of gold and silver from secondary sources of electronic waste processing by thiourea leaching. *JOM* **70**, 1616-1621 (2018).
20. Burdinski, D. & Blees, M. H. Thiosulfate- and thiosulfonate-based etchants for the patterning of gold using microcontact printing. *Chem. Mater.* **19**, 3933-3944 (2007).
21. Cho, E. C., Xie, J., Wurm, P. A. & Xia, Y. Understanding the role of surface charges in cellular adsorption versus internalization by selectively removing gold nanoparticles on the cell surface with a I_2/KI etchant. *Nano Lett.* **9**, 1080-1084 (2009).
22. Parga, J. R., Valenzuela, J. L. & T., F. C. Pressure cyanide leaching for precious metals recovery. *JOM* **59**, 43–47 (2007).
23. Lopes, P. P. *et al.* Dynamics of electrochemical Pt dissolution at atomic and molecular levels. *J. Electroanal. Chem.* **819**, 123-129 (2018).

24. Peng, Y. *et al.* Environmentally Benign, Rapid, and SelectiveExtraction of Gold from Ores and Waste ElectronicMaterials. *Angew.Chem. Int. Ed.* **56**, 9331 – 9335 (2017).

25. Hong, J. *et al.* "Organic Aqua Regia"—Powerful Liquids for Dissolving Noble Metals. *Angew. Chem. Int. Ed.* **49**, 7929 –7932 (2010).

26. Hong, Y. et al. Precious Metal Recovery from Electronic Waste by a Porous Porphyrin Polymer. *PNAS* **117** (28), 16174-16180 (2020).

27. David K. Smith. *et al.* SelectiveExtraction and In Situ Reduction ofPrecious Metal Salts from Model Waste To Generate Hybrid Gels with Embedded Electrocatalytic Nanoparticles. *Angew.Chem. Int. Ed.* **55**, 183 –187 (2016).

28. Wendy L. Queen. *et al.* Rapid, Selective Extraction of Trace Amounts of Gold from Complex Water Mixtures with a Metal−Organic Framework (MOF)/Polymer Composite. *J. Am. Chem. Soc.* **140**, 48, 16697–16703 (2018).

29. Wang, X. *et al.* Semiconductor Heterojunction Photocatalysts: Design, Construction, and Photocatalytic Performances. *Chem. Soc. Rev.* **43**, 5234 (2014).

30. Serhiy, C. *et al.* Dissolution of Noble Metals during Oxygen Evolution in Acidic Media. *ChemCatChem* **6**(8), 2219-2223 (2014).

31. Dong, C. *et al.* Size-dependent activity and selectivity of carbon dioxide photocatalytic reduction over platinum nanoparticles. *Nat. Commun.* **9**, 1252 (2018).

32. Sun, C. & Xue, D. In situ IR spectral observation of $NH_4H_2PO_4$ crystallization: structural identification of nucleation and crystal growth. *J. Phys. Chem. C* **117**, 19146-19153 (2013).

33. Ennis, C., Auchettl, R., Ruzi, M. & Robertson, E. G. Infrared characterisation of acetonitrile and propionitrile aerosols under Titan's atmospheric conditions. *Phys. Chem. Chem. Phys.* **19**, 2915-2925 (2017).

34. Li, Y. H. *et al.* Unidirectional suppression of hydrogen oxidation on oxidized platinum clusters. *Nat. Commun.* **4**, 2500 (2013).

35. Chaudhuri., P. *et al.* Electronic structure of bis(o-iminobenzosemiquinonato)metal complexes (Cu, Ni, Pd). The art of establishing physical oxidation states in transition-metal complexes containing radical ligands. *J. Am. Chem. Soc.* **123**, 2213-2223 (2001).

36. Siemer, N. *et al.* Atomic scale explanation of O_2 activation at the Au-TiO_2 interface. *J. Am. Chem. Soc.* **140**, 18082-18092 (2018).

37. Han, G. *et al.* Visible-light-driven valorization of biomass intermediates integrated with H_2 production catalyzed by ultrathin Ni/CdS uanosheets. *J. Am. Chem. Soc.* **139**, 15584-15587 (2017).

38. Xiao, J. *et al.* Integration of Plasmonic Effects and Schottky Junctions into Metal Organic Framework Composites: Steering Charge Flow for Enhanced Visible-Light Photocatalysis. *Angew. Chem. Int. Ed.* **57**(4), 1103-1107 (2017).

39. Frens, G Controlled Nucleation for the Regulation of the Particle Size in Monodisperse Gold Suspensions. *Nat. Phys. Sci.* **241**, 20-22 (1973).

40. P. C. Lee and D. Melsel. Adsorption and Surface-Enhanced Raman of Dyes on Silver and Gold Sols. *J. Phys. Chem.* **86**, 3391-3395 (1982).

41. Liu, L., Gao, F., Zhao, H. & Li, Y. Tailoring Cu valence and oxygen vacancy in Cu/TiO_2 catalysts for enhanced CO_2 photoreduction efficiency. *Appl. Catal. B-Environ.* **134-135**, 349-358 (2013).

Acknowledgments This work was supported by the National Natural Science Foundation of China (21876114, 21761142011), Shanghai Government (19DZ1205102, 19160712900, 18JC1412900), Chinese Education Ministry Key Laboratory and International Joint Laboratory on Resource Chemistry, and Shanghai Eastern Scholar Program. Shanghai Engineering Research Center of Green Energy Chemical Engineering (18DZ2254200). A patent has been filed to protect the method.

Author Contributions Y.C., M.J.X., Z.F.B. and H.X.L. conceived the idea for the paper. Y.C., Z.F.B. and H.X.L. designed the experiments. Y.C., J.Y.W., Y.W. synthesized the material. Q.F.Z., Y.D., X.C. and Z.L.W. performed the HAADF STEM images. Y.C. performed the sample characterization. Z.F.B., Z.L.W and H.X.L. conducted the experiments. Y.C., Z.F.B. and H.X.L. analyzed the data and wrote the manuscript. All authors contributed to writing the paper.

Competing interests The authors declare no competing interests. Author Information Reprints and permissions information is available at www.nature.com/reprints. Readers are welcome to comment on the online version of the paper. Correspondence and requests for materials should be addressed to Z.L.W. (zlwang@gatech.edu), H.X.L. (hexing-li@shnu.edu.cn) or Z.F.B. (bianzhenfeng@shnu.edu.cn).